



Deposited via The University of Sheffield.

White Rose Research Online URL for this paper:

<https://eprints.whiterose.ac.uk/id/eprint/81373/>

Version: Accepted Version

Article:

Ng, J.S., Meng, X., Lees, J.E. et al. (2014) Fabrication study of GaAs mesa diodes for X-ray detection. *Journal of Instrumentation*, 9. T08005. ISSN: 1748-0221

<https://doi.org/10.1088/1748-0221/9/08/T08005>

Reuse

Items deposited in White Rose Research Online are protected by copyright, with all rights reserved unless indicated otherwise. They may be downloaded and/or printed for private study, or other acts as permitted by national copyright laws. The publisher or other rights holders may allow further reproduction and re-use of the full text version. This is indicated by the licence information on the White Rose Research Online record for the item.

Takedown

If you consider content in White Rose Research Online to be in breach of UK law, please notify us by emailing eprints@whiterose.ac.uk including the URL of the record and the reason for the withdrawal request.

TECHNICAL REPORT

Fabrication study of GaAs mesa diodes for X-ray detection

J.S. Ng,^{a,1} X. Meng,^a J.E. Lees,^b A. Barnett^c and C.H. Tan^a

^a*Department of Electronic & Electrical Engineering, University of Sheffield, Mappin Street, Sheffield, S1 3JD, U.K.*

^b*Space Research Centre, Department of Physics and Astronomy, University of Leicester, Leicester, LE1 7RH, U.K.*

^c*Department of Engineering and Design, School of Engineering and Informatics, University of Sussex, Falmer, Brighton, BN1 9QT, U.K.*

E-mail: j.s.ng@sheffield.ac.uk

ABSTRACT: A study of leakage currents using GaAs mesa p-i-n diodes for X-ray photon counting is presented. Different wet chemical etching solution and etch depth were used in the fabrication of these mesa diodes. Low and uniform leakage currents were achieved when the diode fabrication used (i) a combination of main etching solution and finishing etching solution for the etching, and (ii) partially etched mesas. The diodes fabricated using these methods showed well-defined X-ray peaks when illuminated with an ⁵⁵Fe radioisotope source.

KEYWORDS: Solid state detectors; X-ray detectors; Detector design and construction technologies and materials

¹Corresponding author.

Contents

1	Introduction	1
2	Experimental Details	2
3	Results	4
4	Discussions	7
5	Conclusions	8

1 Introduction

Direct detection using semiconductor devices to convert X-ray photons into electrical charge can be adopted to achieve high spectral resolution. When compared with elemental semiconductors such as Si and Ge, compound semiconductors can be grown with a wide range of physical properties allowing customisation for different applications. Among the III-V compound semiconductors, GaAs has been the most intensively investigated for X-ray detection [1–6]. Its moderately large band gap (1.42 eV) and electron-hole pair creation energy (4.184 ± 0.025 eV [7]) enables room temperature operation, with a potential Fano-limited energy resolution of 129 eV (full-width-half-maximum, FWHM) at 5.9 keV, as calculated using values of pair creation energy and Fano factor from [7]. In addition GaAs has high absorption coefficients, which offers high detection efficiency, due to its high atomic number (Ga = 31 and As = 33) and crystal density (5.3176 g/cm³).

Recently X-ray detectors using avalanche photodiodes (APDs) were found to improve, under certain conditions, the signal-to-noise ratio, particularly at low X-ray energies, experimentally [8] and theoretically [9]. The improvement originates from the APD's avalanche gain, which is the end result of numerous impact ionization events that have taken place in the APD under appropriate conditions. There is however noise from the APD, which can fortunately be minimized if the Separate Absorption and Multiplication APD (SAM-APD) design, as used in optical communication APDs, is adopted [9].

A GaAs-based SAM-APD for X-ray photons will have a GaAs absorption layer and a wide bandgap avalanche layer. Using a wide bandgap material in the avalanche region will enable the use of very thin avalanche layers, which will have better X-ray energy resolution compared to thick avalanche layers, since mixed injection in the avalanche region is minimized [9], while maintaining acceptably low dark current. Several wide bandgap semiconductor alloys with well-characterized impact ionization properties, such as AlGaAs [10, 11], InGaP [12] and AlInP [13], can be grown lattice matched to GaAs.

There have also been efforts in developing the material GaAsBiN, which can also be lattice matched to GaAs [14]. This offers further optimization options since GaAsBiN may offer high absorption efficiency due to the very high atomic number of 84 in Bi.

Despite the promises on performance mentioned above, performance of any GaAs based SAM-APD will be compromised if dark current characteristics of GaAs diodes are not optimized. Furthermore, in X-ray imaging arrays with a mesa structure for the pixel, part or all of the thick undoped GaAs absorption layer between pixels must be etched away, leading to a large surface area that will likely cause significant leakage current. Large variation in the leakage current from pixel to pixel is also highly undesirable as it leads to poor image quality or requires extensive signal processing. Hence it is vital to optimize the fabrication procedures to minimize (i) surface leakage current of thick GaAs mesa diodes, and (ii) variation in leakage current from diode to diode. These are the main contribution of this work, whose application lies in portable medical X-ray detectors [15].

Although GaAs is one of the most studied compound semiconductors, the applications are predominantly focused on lasers and transistors. GaAs X-ray imaging arrays are unique in requiring deep etching (in several microns rather than nanometres) of GaAs to form dense arrays of diodes. The etched diodes' reverse leakage currents are also assessed critically. Possible relevant references are thus quickly narrowed down to those for photodiodes, of which none commercially important ones are made from GaAs. As a result, the relevant references on etching GaAs X-ray diodes are those actually for GaAs X-ray diodes, which are discussed here.

The leakage currents of GaAs X-ray diodes with mesa structures have been reported [1–5]. Although [1] mentioned that etch depth greatly influence the magnitude of leakage current of diodes, very limited information on the wet chemical etchants (type and solution ratio) or dry etching gases (gases' flow rates and sample's temperature) used in etching their GaAs diodes was given in [1–5]. There is no evidence in [1–5] that their GaAs diodes exhibited bulk-only leakage currents.

The very thick ($> 100\ \mu\text{m}$) epitaxially grown GaAs p-i-n diodes of [1] and [2] were produced using wet chemical partial etching without passivation for the mesa. They exhibited dark current density of between $300\ \text{nA}/\text{cm}^2$ to $500\ \mu\text{A}/\text{cm}^2$. Slightly lower dark current density at $100\ \text{nA}/\text{cm}^2$ was achieved in [4]. Later, Kostamo et al. fabricated a GaAs p-i-n diode array using dry etching and passivated the etched diodes with dielectric materials, which yielded dark current density between 40 and $400\ \text{mA}/\text{cm}^2$ [3]. These values are much higher than the dark current density of $5.6\ \text{nA}/\text{cm}^2$ reported by Erd et al. [5], whose array consisted of 32×32 GaAs p-i-n diodes with partially-etched mesa (p layer removed between pixels) and guard rings.

However since then very limited progress in reducing and managing dark current in GaAs has been reported. Hence in this work we report the effects of wet chemical etchants and etch depths on the dark currents of GaAs diodes. X-ray characterisation data using ^{55}Fe is also presented.

2 Experimental Details

The GaAs homojunction p-i-n wafer was grown at the EPSRC National Centre for III-V Technologies at the University of Sheffield. The structure, as summarized in table 1, was grown on a 3-inch GaAs n^+ substrate ($350\ \mu\text{m}$ thick) by metal organic chemical vapor deposition. The p- and n-type dopants used were carbon and silicon.

A series of five samples, namely samples A, B, C, D, and E, was fabricated from the wafer. First, Ti/Au (20/200 nm) were deposited onto the samples, which were then annealed in a rapid thermal annealer at 420°C for 60 s to form ohmic p- and n-contacts. Chemical etching was then

Table 1. Structure details of the GaAs p-i-n wafer.

Material	Thickness (nm)	Type	Doping density (cm^{-3})
GaAs	10	p^+ (C)	1×10^{19}
GaAs	500	p^+ (C)	2×10^{18}
GaAs	7000	i	undoped
GaAs	1000	n^+ (Si)	2×10^{18}
GaAs substrate	—	n^+	—

Table 2. Summary of the five samples.

Sample	Chemical etchants	Etch depth (nm)	Remark
A	$\text{H}_3\text{PO}_4:\text{H}_2\text{O}_2:\text{H}_2\text{O}$	8300	Fully etched
B	$\text{H}_3\text{PO}_4:\text{H}_2\text{O}_2:\text{H}_2\text{O}$ and $\text{H}_2\text{SO}_4:\text{H}_2\text{O}_2:\text{H}_2\text{O}$	8300	Fully etched
C		1000	Partially etched
D	2000		
E	2500		

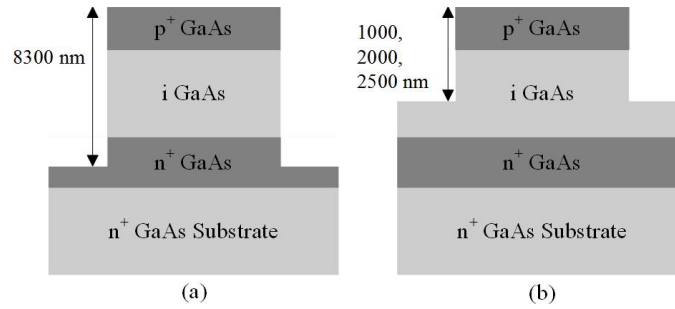


Figure 1. GaAs p-i-n diodes with (a) fully, or (b) partially etched circular mesas.

used to create circular mesas with diameters, d , of 400, 200, 100 and 50 μm . The five samples differ in the chemical etchant used and/or the etch depth (as measured from the top of the wafer), as summarized in table 2. No surface passivation was used in the samples, in order to avoid possible variation in leakage currents due to the passivation material/process used, which will unnecessarily complicate analyses of leakage currents. Surface passivation optimization for thick mesa is beyond the scope of this work.

While the mesas in all samples were created using a solution of phosphoric acid: hydrogen peroxide: deionized water ($\text{H}_3\text{PO}_4:\text{H}_2\text{O}_2:\text{H}_2\text{O} = 1:1:1$) to achieve the intended etch depths, samples B to E had an additional finishing etch using a solution of sulphuric acid: hydrogen peroxide: deionized water ($\text{H}_2\text{SO}_4:\text{H}_2\text{O}_2:\text{H}_2\text{O} = 1:8:80$) for 10 s. Samples A and B have fully etched mesas whereas samples C, D, and E have partially etched mesas of 1000 nm, 2000 nm and 2500 nm respectively, as depicted in figure 1a and figure 1b, respectively. No substrate removal was carried out.

The sulphuric acid-based finishing etch was included in our study because it was found to improve reverse leakage currents of mesa diodes made of InAs [16]. Note that relying on sulphuric acid-based solution for deep etching is generally avoided as it is known to produce anisotropic etch

profiles [17], which affected the circular geometry (to avoid surface leakage current and premature edge breakdown) in our diodes in preliminary etching trials. The ratios for the phosphoric acid-based etchant were chosen to achieve a sufficiently high yet controllable etch rate, following etching trials with a few other ratios.

On-wafer measurements of Current-Voltage (I-V) and Capacitance-Voltage (C-V) characteristics were performed to select promising devices to be packaged for subsequent X-ray measurements. An I-V setup with a Keithley 236 source-measure-unit was used to measure leakage currents ranging from 0.1 pA to 10 mA. The samples were measured at room temperature and in a dark environment to minimize photocurrent generated by stray light. Most of the I-V data were obtained from $d = 200$ and $400 \mu\text{m}$ diodes because these sizes are more relevant to the targeted application. C-V measurements were carried out using a HP 4275A Multi-Frequency LCR Meter with a sinusoidal test signal of 60 mV rms magnitude and 1 MHz frequency. The data allow determination of the minimum reverse bias required to fully deplete the i-GaAs layer.

For preliminary evaluation of the diodes' performance when imaging high energy X-ray photons, packaged GaAs p-i-n diodes were individually tested with a ^{55}Fe source. The diodes were reverse biased at 10 V using a Thurlby Thandar PL330QMD stabilized power supply. The preamplifier used a Si JFET (Vishay Siliconix 2N4416, capacitance ~ 2 pF) for the first transistor. Output from the preamplifier was connected to an Ortec 571 shaping amplifier (shaping time constant $1 \mu\text{s}$), whose output was fed into an Ortec Easy-MCA-8k multichannel analyzer (MCA). An ^{55}Fe radioisotope source (activity of 1.2 GBq) giving Mn $K\alpha$ and $K\beta$ X-ray lines (at 5.9 and 6.5 keV) was positioned 3 mm from the top side of the diode-under-test. The system was kept at room temperature.

3 Results

Typical C-V data for $d = 400 \mu\text{m}$ diodes are shown in figure 2a, which also includes the depletion width versus V deduced from the data. We found very similar C-V data for same-sized diodes from the different samples, when $V > 10$ V. For example, at reverse bias of 15 V, capacitance values of $400 \mu\text{m}$ diameter diodes were between 1.99 and 2.15 pF, within the tolerance of the measurement setup. This similarity indicates negligible unwanted lateral depletion in the diodes and hence complete isolation of the diodes.

Observing figure 2a, analyses of the C-V data also revealed that the i-GaAs layer thickness is $\sim 6.7 \mu\text{m}$, slightly thinner than the intended value of $7.0 \mu\text{m}$. The deviation was confirmed by data from Secondary Ion Mass Spectroscopy, as shown in figure 2b, carried out elsewhere on the wafer. The thinner than intended i-GaAs layer is likely to be due to a combination of slight uncertainty in growth rate and dopant diffusion from the highly-doped p- or n-layer into the i-layer, which had taken place during the epitaxial growth. Note that as the instrument background of this measurement is high for carbon ($\sim 2 \times 10^{16}$ atom/cm³), exact extent of carbon diffusion from the p-layer into the i-layer could not be accurately determined.

To observe if the finishing etch had any noticeable effect on the leakage current, leakage current density of the two samples with fully etched mesas are compared in figure 3a. Data of 35 diodes (23 of $d = 200 \mu\text{m}$ and 12 of $d = 400 \mu\text{m}$) are shown for each sample. We found that sample A exhibited moderately uniform but high leakage current density, whereas sample B generally

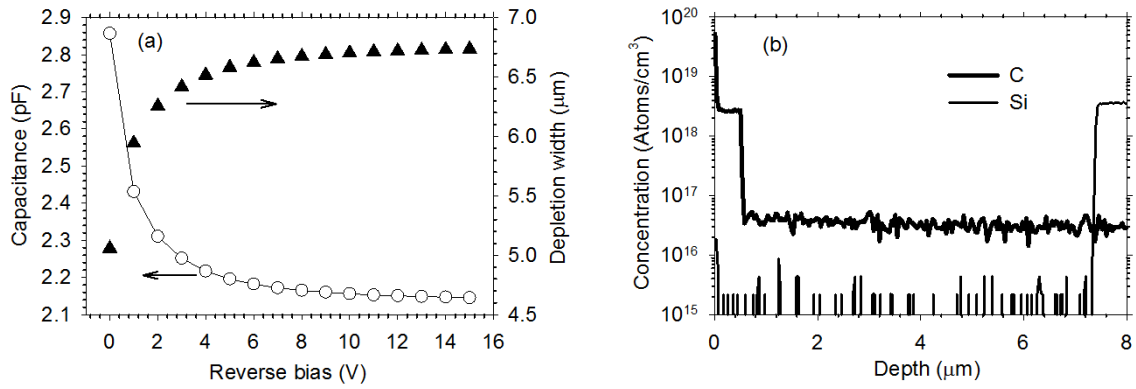


Figure 2. (a) Typical C-V data (right axis, circles) and deduced depletion width (right axis, triangles) of a $d = 400 \mu\text{m}$ p-i-n diodes. (b) Secondary Ion Mass Spectroscopy data showing the p (carbon) and n (silicon) doping profiles of the GaAs p-i-n wafer.

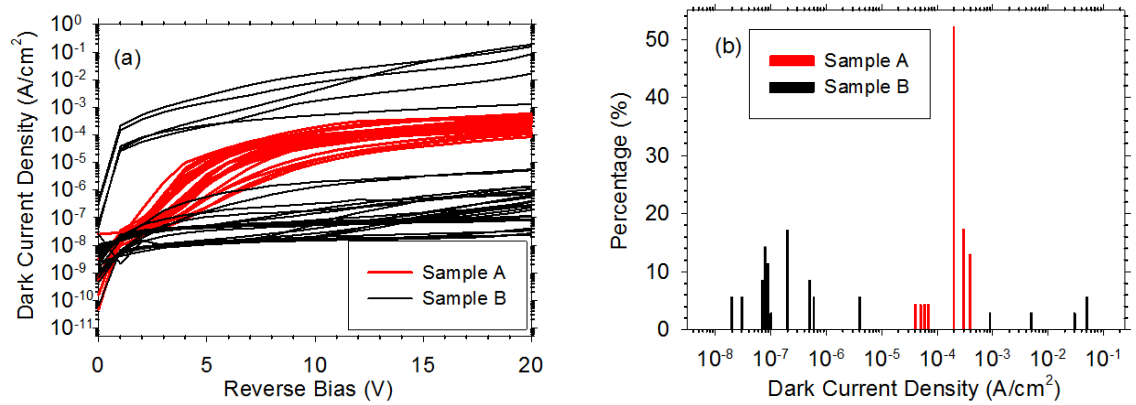


Figure 3. (a) Dark current density versus reverse bias, and (b) distribution of dark current density at 15 V for samples A and B, which have fully etched mesas. Sample B had the additional finishing etch of $\text{H}_2\text{SO}_4:\text{H}_2\text{O}_2:\text{H}_2\text{O}$. There were 23 and 12 diodes with diameters of $200 \mu\text{m}$ and $400 \mu\text{m}$ diodes, respectively.

had lower leakage current density (10 to $100 \text{ nA}/\text{cm}^2$) although some diodes were very poor (1 to $10 \text{ mA}/\text{cm}^2$). In figure 3b, we compare the distribution of leakage current density at 15 V for samples A and B. Although sample B had a wider distribution than sample A, $\sim 46\%$ of the diodes tested in sample B had leakage current density $< 0.1 \mu\text{A}/\text{cm}^2$, with some having current densities as low as $20 \text{ nA}/\text{cm}^2$. Hence the finishing etch appears to reduce leakage currents in diodes with fully etched mesas. Note that as the current does not scale with diode area, the measured current was dominated by surface leakage current component.

Since samples C, D, and E all had a finishing etch for their partially-etched mesas with different etch depths of 1000 nm, 2000 nm and 2500 nm respectively, they can be studied to observe effects of etch depth on the leakage current density and its distribution. Figure 4a and figure 4b compare their leakage current densities, and distributions of leakage current, based on data of 12 diodes (8 of $d = 200 \mu\text{m}$ and 4 of $d = 400 \mu\text{m}$) from each sample. Among these three samples, sample D

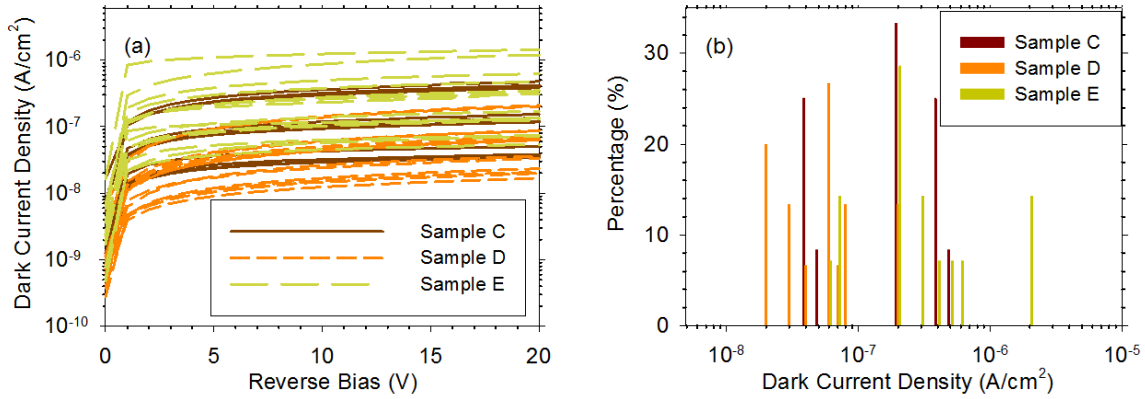


Figure 4. (a) Dark current density versus reverse bias, and (b) distribution of dark current density at 15 V for samples C, D, and E, which have partially etched mesas. There were 8 and 4 diodes with diameters of 200 μm and 400 μm diodes, respectively.

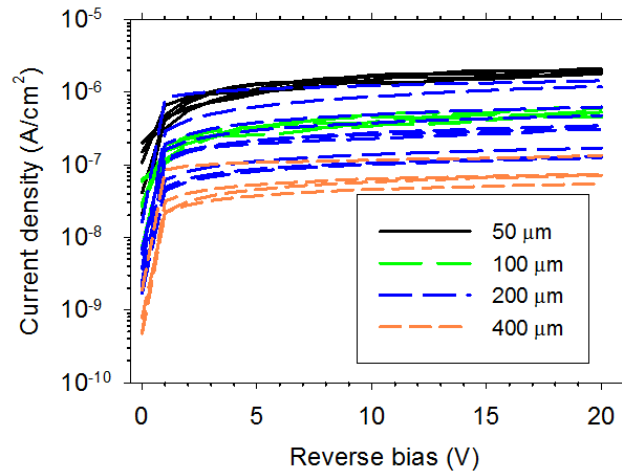


Figure 5. Dark current density versus reverse bias for 6, 6, 8, and 4 diodes with diameters of 50, 100, 200, and 400 μm , respectively, from sample E.

exhibited the lowest leakage current densities, with 75% of the diodes tested having dark current density $< 100 \text{ nA/cm}^2$ and a very low mean dark current density of 20 nA/cm^2 for $d = 400 \mu\text{m}$ diodes. This compares favorably to mean leakage current densities of samples C and E, at 40 and 80 nA/cm^2 , respectively (for $d = 400 \mu\text{m}$ diodes).

For a given sample, comparisons of leakage current density from different sized diodes were made and the data from sample E are shown as an example in figure 5. As the diode's diameter and hence junction area decreased, the leakage current density increased, indicating that sidewall-related leakage current became increasingly significant compared to the bulk-related leakage current.

Figure 6 shows an ⁵⁵Fe X-ray spectrum accumulated over 60 s with a 400 μm diameter diode from sample B. The diode was reverse biased at 10 V (depletion width of $\sim 6.7 \mu\text{m}$), to maintain a low leakage current of 0.3 pA. The spectral resolution, as given by the FWHM of the combined 5.9 keV and 6.5 keV peaks is 1.0 keV.

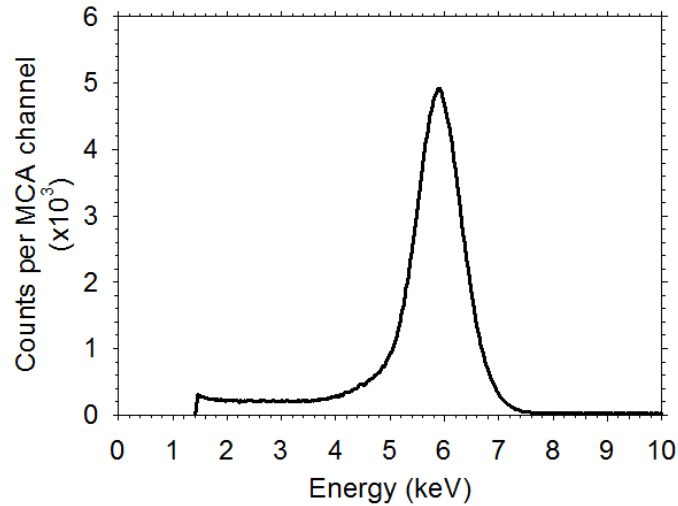


Figure 6. An ^{55}Fe X-ray spectrum accumulated with a diode over 60 s. The count rate was 1.2×10^4 counts per second in the energy range of 1.35 keV to 8 keV.

4 Discussions

Our work on diodes with fully etched mesas showed that using only a solution $\text{H}_3\text{PO}_4:\text{H}_2\text{O}_2:\text{H}_2\text{O}$ for etching produces high surface leakage currents in the resultant diodes. Adding a finishing etch using a solution of $\text{H}_2\text{SO}_4:\text{H}_2\text{O}_2:\text{H}_2\text{O}$ can substantially lower the surface leakage currents although the uniformity is still not satisfactory. The variation of dark currents of fully etched diodes on sample B is undesirable for a detector array since it would lead to a large proportion of non-useable pixels. This variation may be caused by variation in surface states on the sidewalls of the mesas, which may be reduced if mesa passivation optimized for GaAs X-ray diodes is available.

The partially etched diodes suffer from this problem at a much lower extent, because the mesa sidewalls are much shorter, resulting in significantly smaller exposed area on the mesa sidewalls. The mean dark current density of sample D at 20 nA/cm^2 (for $d = 400 \mu\text{m}$ diodes) is much lower than those from refs. [1–4], but is slightly higher than one of the lowest dark current densities in the literature, 5.6 nA/cm^2 at 50 V at room temperature [5]. The very low dark current density in [5] might be due to the use of guard rings, which can help to suppress surface leakage currents. Nevertheless our results demonstrated that, by adopting appropriate chemical etchants ($\text{H}_3\text{PO}_4:\text{H}_2\text{O}_2:\text{H}_2\text{O}$ followed by $\text{H}_2\text{SO}_4:\text{H}_2\text{O}_2:\text{H}_2\text{O}$) and etch depth, low leakage currents with good uniformity can be achieved for progress towards detector array.

Although each of our three samples with partially etched diodes show reasonably uniform dark currents, the mean dark currents from the three samples do differ in magnitude. While this observation is consistent with previous works [1–3], there has been no discussion on this in the literature. Hence it is worthwhile analyzing our data for partially etched diodes further. Sample C had an etch depth of 1000 nm for a wafer designed to have 510 nm of p-type layer. This would have removed all p-type material between the diodes, thus achieving good level of isolation between the diodes. However, a variation in the etch depth across the sample and dopant diffusion from the p-layer into the i-layer may mean having conducting path along some remaining thin p-type mate-

rial between the diodes. This will compromise isolation between the diodes and cause additional leakage currents. Therefore a more reliable etch depth would be one that is deeper than the p-type layer thickness by some margins.

For sample E, its higher leakage current density (compared to that of sample D) is probably due to the advantage of reduced surface damage in partially etch diode being lost as the etch depth increases to 2500 nm.

In our X-ray measurement, the FWHM of 1.0 keV is far from the Fano limited case of 129 eV at 5.9 keV at room temperature and the best experimental reports (266 eV FWHM at 5.9 keV [6]). The noise beyond the Fano limit reported here is due to a combination of electronic noise (including parallel white, series white, dielectric, and 1/f noise) from both the preamplifier [18] and detector, and also possibly charge trapping noise [19]. Full shaping time noise analysis of these noise sources and the contributions to the achievable energy resolution is planned for future work. If the reported photodiodes are to be practical options for use in high energy resolution X-ray spectroscopy in the future, the achievable energy resolution must be improved by reducing these noise contributions. However, the detectors reported here are part of early development for imaging arrays, where the energy resolution requirements are more modest.

5 Conclusions

Our work demonstrated that the surface leakage current of diodes with mesa structures can be reduced by adopting appropriate chemical etchants and partially etched mesa. Our best sample, which has partially etched mesas showed uniformly low dark currents, with a low mean value of 20 nA/cm².

Acknowledgments

This work was supported by the U.K. Science and Technology Facilities Council under Grants ST/H000127/1 and ST/H000143/1. The work of J.S. Ng was supported by the Royal Society University Research Fellowship. The authors thank Dr. J. Xie, Dr. S. Xie, and Dr. N. Babazadeh for assistance in device fabrication as well as Dr. B.J. Stevens for wafer growth.

References

- [1] H. Samic et al., *Characterization of Thick Epitaxial GaAs Layers for X-ray Detection*, *Nucl. Instrum. Meth. A* **487** (2002) 107.
- [2] G.C. Sun et al., *X-ray detector with thick epitaxial GaAs grown by chemical reaction*, *IEEE Trans. Nucl. Sci.* **50** (2003) 1036.
- [3] P. Kostamo et al., *GaAs Medipix2 hybrid pixel detector*, *Nucl. Instrum. Meth. A* **591** (2008) 174.
- [4] G.I. Ayzenshtat et al., *X-ray and γ -ray detectors based on GaAs epitaxial structures*, *Nucl. Instrum. Meth. A* **531** (2004) 97.
- [5] C. Erd et al., *Hard X-ray test and evaluation of a prototype 32×32 pixel gallium-arsenide array*, *Nucl. Instrum. Meth. A* **487** (2002) 78.

- [6] A. Owens et al., *High resolution x-ray spectroscopy using GaAs arrays*, *J. Appl. Phys.* **90** (2001) 5376.
- [7] G. Bertuccio and D. Maiocchi, *Electron-hole pair generation energy in gallium arsenide by x and γ photons*, *J. Appl. Phys.* **92** (2002) 1248.
- [8] R.B. Gomes, C.H. Tan, P.J. Ker, J.P.R. David and J.S. Ng, *InAs avalanche photodiodes for X-ray detection*, 2011 *JINST* **6** P12005.
- [9] C.H. Tan et al., *Avalanche Gain and Energy Resolution of Semiconductor X-ray Detectors*, *IEEE Trans. Electron Dev.* **58** (2011) 1696.
- [10] C.H. Tan, J.P.R. David, S.A. Plimmer, G.J. Rees, R.C. Tozer and R. Grey, *Low Multiplication Noise Thin $Al_{0.6}Ga_{0.4}As$ Avalanche Photodiodes*, *IEEE Trans. Electron Dev.* **48** (2001) 1310.
- [11] B.K. Ng, J.P.R. David, R.C. Tozer, M. Hopkinson, G. Hill and G.J. Rees, *Excess Noise Characteristics of $Al_{0.8}Ga_{0.2}As$ Avalanche Photodiodes*, *IEEE Photon. Tech. Lett.* **14** (2002) 522.
- [12] C.H. Tan, R. Ghin, J.P.R. David, G.J. Rees and M. Hopkinson, *The effect of dead space on gain and excess noise in $In_{0.48}Ga_{0.52}P$ p^+in^+ diodes*, *Semicond. Sci. Technol.* **18** (2003) 803.
- [13] J.S.L. Ong, J.S. Ng, A.B. Krysa and J.P.R. David, *Impact ionization coefficients in $Al_{0.52}In_{0.48}P$* , *IEEE Electron Dev. Lett.* **32** (2011) 1528.
- [14] S.J. Sweeney and S.R. Jin, *Bismide-nitride alloys: promising for efficient light emitting devices in the near- and mid-infrared*, *J. Appl. Phys.* **113** (2013) 043110.
- [15] E.N. Ardashev, S.A. Gorokhov, M.K. Polkovnikov, I.S. Locanov and A.P. Vorobiev, *A portable X-ray apparatus with GaAs linear array*, *Nucl. Instrum. Meth. A* **648** (2011) S8.
- [16] A.R.J. Marshall, *The InAs electron avalanche photodiode and the influence of thin avalanche photodiodes on receiver sensitivity*, Ph.D. Thesis, University of Sheffield, (2009), chapter 3, pg. 46.
- [17] A. Baca and C. Asby, *Fabrication of GaAs Devices*, *The Institution of Electrical Engineers*, London, U.K. (2005), chapter 4, pg. 133–134.
- [18] A.M. Barnett, J.E. Lees, D.J. Bassford and J.S. Ng, *A varied shaping time noise analysis of $Al_{0.8}Ga_{0.2}As$ and GaAs soft X-ray photodiodes coupled to a low-noise charge sensitive preamplifier*, *Nucl. Instrum. Meth. A* **673** (2012) 10.
- [19] A. Owens and A. Peacock, *Compound semiconductor radiation detectors*, *Nucl. Instrum. Meth. A* **531** (2004) 18.